THE JOURNAL OF PHYSICAL CHEMISTRY B

Article

pubs.acs.org/JPCB

Atomistic Description of the Solubilisation of Testosterone Propionate in a Sodium Dodecyl Sulfate Micelle

Daniel T. Allen,[†] Yussif Saaka,[‡] M. Jayne Lawrence,[‡] and Christian D. Lorenz*[,†]

[†]Theory & Simulation of Condensed Matter Group, Department of Physics, Strand Campus, King's College London, Strand, London WC2R 2LS, England

[‡]Pharmaceutical Biophysics Group, Institute of Pharmaceutical Science, King's College London, Franklin-Wilkins Building, 150 Stamford Street, London SE1 9NH, England

Supporting Information

ABSTRACT: Large-scale molecular dynamics simulations were used to study the structural and dynamic properties of the solubilization process of testosterone propionate (TSTP) within sodium dodecyl sulfate (SDS) micelles. We observed that the TSTP spontaneously adsorb onto the SDS micelles and preferentially reside among the polar head groups of the SDS molecules. We found that the SDS micelle is slightly aspherical in size and has a surface area of ∼170 Å^2/molecule, while the SDS+TSTP micelle is more aspherical and has a surface area of ∼156 Å^2/molecule. The structural properties of the interior of the SDS micelle and the hydration of the SDS headgroup are largely undisturbed by the presence of the TSTP. However, there seems to be a correlation between the location of the TSTP molecules and the location of Na^+ counterions on the surface of the SDS micelle. Additionally, we also observe that the TSTP molecules diffuse on the surface of the SDS micelle and try to organize themselves such that they are approximately equidistant from one another.

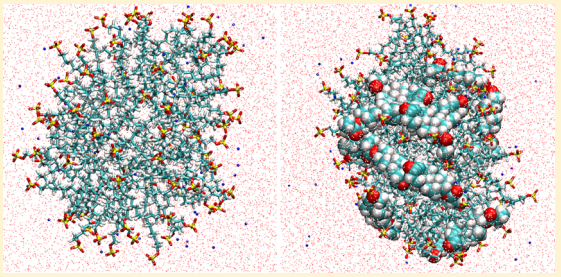

INTRODUCTION

Amphiphilic molecules consist of polar head groups and nonpolar tails. Because of this chemical composition, amphiphilic molecules are known to spontaneously self-assemble into a variety of aggregate structures when their concentration in water exceeds the critical micelle concentration (CMC). Such self-assembled structures include micelles, bilayers, lamellar, and other cubic phases. The hydrophobic microenvironment, arising from the hydrophobic interior of an aggregate, can increase the apparent aqueous solubility of other, slightly soluble nonpolar substances. This phenomenon is known as "solubilization" and is imperative to many biological and industrial processes.

A wide-range of surfactants have been investigated as the building blocks of nanoscale drug delivery vehicles due to the solubilizing ability of the self-assembled structures that they form (see refs 1−3 and the references within each). Specifically, sodium dodecyl sulfate (SDS, $SO_4(CH_2)_{11}CH_3$, shown in Figure 1a) has a relatively low toxicity compared to other surfactants and is used for many industrial applications, including in the pharmaceutical industry as a wetting and solubilizing agent in tablet formulations.

Numerous research groups have applied experimental techniques to characterize the solubilization of various drug molecules within SDS micelles. Krishna and Flanagan used UV detection to determine that SDS significantly solubilizes the antimalarial drug, β-arteether.[4] On the other hand, Rangel-Yagui et al. observed that SDS is less effective than nonionic or cationic surfactants with the same hydrocarbon chain length in solubilizing ibuprofen.[5] Mall et al. measured the free energy of adhesion between four different sulphanmides and the head and tail groups of SDS using contact angle data, and found that the most favored interaction was adhesion to the SDS tails, as opposed to an interaction with the head groups.[6] A similar finding has been presented as a result of the conductivity, spectroscopy, and surface tension measurements carried out by Göktürk and Aslan that show an increase in trimetoorim binding as the length of the hydrocarbon chain in sulfate anionic surfactants increases, which led them to hypothesize that the increased binding is due to there being more hydrophobic volume for the drug molecules in the micelles.[7] Whereas, Enache et al. used UV−vis adsorption and voltammetry experimental results to develop the hypothesis that the anticancer drug, mitoxantrone, is located in the micelle surface layer as a result of both electrostatic and polar interactions playing an important role in the binding of the drug to SDS micelles.[8]

Since SDS aggregates in aqueous environments have spatial length scales which are typically a few nanometers, it is challenging for experimental research to capture a direct view of the poorly water-soluble substance under investigation. Furthermore, details regarding micellar structure on an atomic

Received: August 22, 2014
Revised: October 22, 2014
Published: October 24, 2014

   dx.doi.org/10.1021/jp508488c | J. Phys. Chem. B 2014, 118, 13192−13201

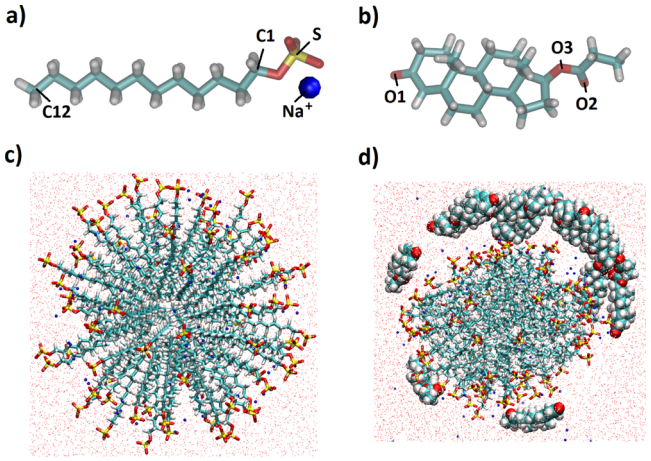

Figure 1. (a) Chemical structure of SDS. (b) Chemical structure of testosterone propionate. Initial configurations of the SDS and SDS +TSTP micelles are shown in (c and d), respectively. In the snapshots in (c and d), the water molecules are represented as points in order to make the other components of the system more clear to see. In all figures, the colors cyan, gray, red, yellow, and blue are used to represent the elements: carbon, hydrogen, oxygen, sulfur, and sodium, respectively.

scale are hardly accessible by experimental techniques. However, molecular dynamics (MD) simulations have been utilized to study many surfactant aggregate systems, including SDS. In these studies, MD simulations provide an important compliment to experimental studies because they yield atomistic level insight into the structure and dynamics of the surfactant systems. Atomistic detail can provide insight on interactions between specific atoms or functional groups which in turn can be used to form a physical explanation for the qualitative behavior observed. If we can probe the interactions which result in the solute's positioning then we can also predict the preferential position of other solutes in micelles and assess the practical potential of a given drug delivery vehicle.

A significant amount of simulation work has been carried out over the years investigating various structural, interfacial, and kinetic properties of SDS micelles using MD simulations. The first simulation study of a SDS micelle was published in 1990, in which a 182 ps simulation showed that a micelle containing 42 SDS molecules was spherical in shape and an initial investigation of the structural and interfacial properties of the micelle was carried out.[9] In 1995, MacKerell published the results of a 120 ps simulation of a micelle consisting of 60 SDS molecules, which showed that it was spherical in shape also and that both headgroup atoms and terminal carbons were present at the micelles interface with water.[10] Bruce et al. conducted a 5 ns simulation of a micelle with 60 SDS molecules which resulted in them finding a slightly nonspherical micelle, and they measured the surface area of the micelle, the orientation of the SDS chains within the micelle, and the interactions between the SDS headgroup and water and Na^+ ions at the micelle's interface.[11,12] Since these four initial simulation studies, various simulation studies have been conducted studying the interfacial properties of SDS micelles in an aqueous environment,[13−17] as well as the effect that the type of counterion,[13] the concentration of ions in the system[18] and the number of SDS molecules in a micelle[19] has on the structural and interfacial properties of the micelles. Additionally, some work has been done to study the aggregation of SDS micelles at high SDS concentrations (∼1 M).[18,20] Recently, a comparison of the various force fields that exist to study SDS micelles in an aqueous environment has been reviewed and found that only for large (aggregation number of ∼100 SDS molecules) micelles does the force field have a significant difference.[21]

Despite the abundant use of MD simulations to study the structural and interfacial properties of SDS micelles, there is a distinct lack of work regarding the solubilization properties of drug molecules within SDS micelles. Yan et al.[22] assessed the structural and dynamical aspects of the solubilization process of pyrene within a sodium dodecyl sulfate micelle using MD simulations. They observed that a free pyrene fluorescence probe was spontaneously solubilized into the SDS micelle and preferentially resides in the hydrophobic core region. As the local concentration of pyrene was increased, two probe molecules could enter the hydrophobic core region and an excited dimer of pyrene molecules was formed which shortly separated and the pyrene molecules were later found to be distributed in the micelle palisade layer. More recently, groups have been utilizing the structure of surfactant (including SDS) micelles in combination with COSMOmic to determine the partitioning and free energy of adsorption of drug molecules within the micelles, which allows for a relatively fast way of determining the most probable location of a drug molecule but does not provide any direct information regarding the interactions which govern the encapsulation of the drugs within the micelle.[23,24]

In this study, we present results from large scale all-atom MD simulations of SDS micelles with and without testosterone propionate (TSTP). TSTP is a steroid which is used in hormone replacement therapy for individuals who have abnormally low testosterone levels. Little is known regarding the interactions between TSTP and the solubilizing agents used to enhance its aqueous solubility, in particular, the location of solubilized TSTP in relation to an SDS micelle is unknown. The chemical structure of TSTP consists of both hydrophobic and hydrophilic functional groups, and as a result, the location of solubilized TSTP in a micelle is difficult to predict. Moreover, testosterone has several analog compounds, such as testosterone enanthate, which have different functional groups but comparable molecular weights. The study of this group of compounds should provide insight into the key interactions which govern solubilized position of solutes in micelles.

We investigate how TSTP influences micelle structure, shape, and interfacial properties as it is solubilized into a SDS micelle. We also provide a detailed description of the TSTP solubilization process.

The rest of the manuscript is organized as follows. In Simulation Methods, we summarize our simulation model and computational techniques employed. In Results and Discussions, we present the results of our simulations and specifically discuss (i) an atomistic description of the solubilization process of TSTP into an SDS micelle, (ii) the effect of TSTP on SDS micelle shape and structure, and (iii) the effect of TSTP on SDS micelle interfacial properties. In Conclusions, we discuss our results in comparison to other findings of SDS micelles and outline our aspirations for future work.

SIMULATION METHODS

All-atom MD simulations have been used to investigate how the presence of TSTP affects the structural and interfacial

dx.doi.org/10.1021/jp508488c | J. Phys. Chem. B 2014, 118, 13192−13201

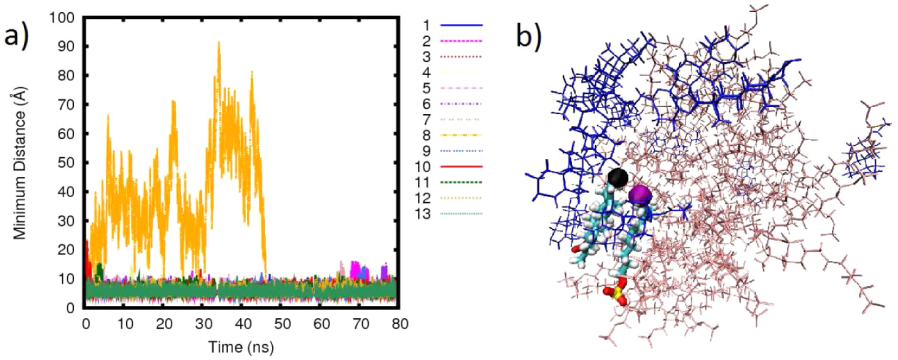

Figure 2. (a) The minimum distance between any sulfur atom in a SDS molecule and the O1 atom of each TSTP molecule (as shown in Figure 1) as a function of time. The plot shows that one of the TSTP molecules does not adsorb to the micelle's surface until after 45 ns. (b) Snapshot of an instance when the O1 atom of a TSTP molecule is closest to a C12 atom in a SDS molecule, which is at the surface of the micelle. The SDS and TSTP molecules are represented by pink and blue lines, respectively. The purple and black spheres represent the C12 on the SDS molecule and the O1 atom on the TSTP molecule, respectively.

properties of a SDS micelle in an aqueous solution. In these simulations, we have used the results from recent neutron scattering experiments to determine the number of SDS and TSTP molecules within a micelle. The aggregation numbers determined from the neutron scattering experiments are 80 SDS molecules for the SDS micelle and 76 and 13 molecules of SDS and TSTP, respectively, for the SDS+TSTP micelle. Further details of these experimental studies will be presented in future papers. However, there is a brief explanation of the measurements and the results of the fitting of the data in the Supporting Information.

We report results from two systems which were simulated, one with only SDS and water and another with SDS, TSTP, and water (systems will be referred to as SDS and SDS+TSTP, respectively, throughout the remainder of the manuscript). The first system was used so that a SDS micelle alone in an aqueous solution could be studied. The system was initially composed of 80 SDS monomers that are preassembled into a spherical aggregate using Packmol,[25] as is shown in Figure 1c. The preassembled aggregate was then thermalizd in vacuo by first conducting an energy minimization simulation followed by a NVT simulation in which the temperature was held constant at 300 K for 240 ps. After the thermalisation stage, the aggregate was placed into the center of a 126 × 126 × 126 Å simulation box with 64083 water molecules, which results in the concentration of the SDS in the solution being the same as that used in the neutron experiments (3 g/100 mL). We have applied a similar approach previously to study surfactant micelles in the presence of oil molecules.[26]

Then the structure of the hydrated SDS micelle was minimized in order to remove any clashes between water molecules and SDS molecules. Then the system was thermalizd by employing an NVT simulation for 20 ps. Finally, the pressure within the system was equilibrated to 1 atm using the NPT ensemble for 20 ns.

The second system was built so a TSTP-containing SDS micelle can be studied. First, a micelle containing 76 SDS monomers was preassembled using Packmol[25] in a similar fashion as the first system. The micelle was then minimized and thermalizd in vacuo in an identical manner as was used for the SDS micelle system. Next the thermalized micelle was placed within a box of water large enough to make the resulting concentration of SDS to be 3 g/100 mL (same as in neutron experiments). Another energy minimization was performed on the solvated micelle system, after which the system was thermalizd at 300 K using a NVT simulation which was 400 ps in duration.

After allowing the micelle to form the initial intermolecular interactions that stabilize it in solution, we introduced the TSTP molecules into the system. In order to minimize disruption to the interfacial water layer, the SDS aggregate and all water molecules within 5 Å of the aggregate interface were kept from the final configuration of the thermalisation simulation. Then, 13 TSTP molecules were placed just outside the interfacial water layer, ensuring that they were within the interaction cutoff radius of 10 Å from the micelle surface, as shown in Figure 1d. Water molecules were reinserted into the simulation box to ensure that the total number of water molecules in the system was equal to that of the system before the addition of TSTP. The resulting system was subjected to an energy minimization simulation, followed by three further equilibration stages. First, a simulation was carried out in order to equilibrate the pressure of the new system to 1 atm using the NPT ensemble for 2 ns. Next, the temperature was equilibrated at 300 K by running a NVT simulation for 100 ps. Finally, a NPT simulation was performed for 20 ns.

The resulting SDS micellar and SDS+TSTP micellar systems were used to carry out the production simulations, which were performed using the NPT ensemble at a temperature of 300 K and atmospheric pressure and run for 80 ns. All simulations were performed using the LAMMPS simulation package[27] with the CHARMM force field[28,29] for the description of both inter- and intramolecular interactions of the SDS[30,31] and TSTP.[28] The TIP3P water model,[32] which was modified for the CHARMM force field,[33] was used to describe interactions involving water. The van der Waals interactions were cutoff at 10 Å while the electrostatic interactions were cutoff at 12 Å. The PPPM method[34] was used to compute long-range Coulombic interactions. The LAMMPS implementation[35−38] of the Nosé−Hoover thermostat[39] was used to fix the system temperature in all simulations, while the system pressure was controlled using a Nosé−Hoover barostat[40] in the NPT simulations. A time step of 2 fs was used in all production simulations to ensure stable integration of Newton's equations of motion with the velocity Verlet algorithm while all hydrogen-containing bonds were constrained using the SHAKE algorithm.[41] The measurements discussed in the following sections were conducted using the entirety of the 80 ns

dx.doi.org/10.1021/jp508488c | J. Phys. Chem. B 2014, 118, 13192−13201

production periods for both simulations in which the systems were deemed to be stable throughout, based upon stability of the eccentricity and solvent accessible surface area measurements.

RESULTS AND DISCUSSION

In this section, we present the results from all-atom simulations of SDS and SDS+TSTP micelle systems. First we provide a detailed description of the TSTP solubilization process. Then, we present how the presence of TSTP affects the shape and structure of the SDS micelle. Finally, we report how the interfacial properties of the SDS micelle alter with the presence of TSTP.

Atomistic Description of the Solubilization Process of TSTP into an SDS Micelle. The first step in understanding how the SDS micelles solubilize the TSTP molecules is to establish the preferred position of a TSTP molecule with respect to the micelle. In order to do so, we first determined the minimum distance between the O1 atoms of the TSTP molecules and the sulfur in any SDS molecule as a function of time, which is plotted in Figure 2a. Most of the O1 atoms in TSTP molecules are found at a distance of ∼4−10 Å from a sulfur atom for the entirety of the production period. From visual inspection of the trajectory, we observe that most of the TSTP molecules are oriented such that the major axis is at a tangent to the micelle surface and the SDS head groups are very dynamic. The TSTP molecules are typically located between several SDS head groups that periodically sway toward and away from the TSTP, resulting in the ∼6 Å fluctuations in the distances between TSTP and the nearest SDS molecules as shown in Figure 2a. All but one of the TSTP molecules are bound to the SDS micelle from the beginning of the production simulation and the one unbound TSTP molecule adsorbs to the micelle's surface after 45 ns, which is evident by the orange curve which fluctuates significantly throughout the first 45 ns of the trajectory and then reaches the same value of ∼4−10 Å. For this reason, that particular TSTP molecule is only used for the remaining analysis after the point that it adsorbs to the surface of the micelle.

To obtain a statistical description of the position of TSTP molecules in relation to the micelle with atomistic detail, we calculated the probability that a given heavy atom (non-hydrogen) in the SDS molecules is closest to an oxygen atom in TSTP, which is plotted in Figure 3. This probability was determined by first calculating the minimum distance between any SDS heavy atom and any of the three oxygen atoms in the bound TSTP molecules and keeping a tally of the heavy atom in the SDS molecule and the oxygen atom in the TSTP molecule that were closest. This information was then converted to a histogram which is normalized such that the sum of the integrals under the curves representing the three oxygen atoms in TSTP sum to 1.

Figure 3 shows that O1 and O2 atoms in TSTP are most likely to be situated nearest to the SDS headgroup, with a sharp decrease in probability at C1 and then a gentle decay as one moves further down the SDS carbon chain before a slight rise at C11 and C12, the terminal carbons. The probability of sulfur being the closest heavy atom in SDS to any of the oxygens in a TSTP molecule is zero due to the steric and electrostatic energy barriers arising from the three oxygens which surround it. TSTP-O3 is most likely to be closest to C12 in SDS but has very low probability of being closest to the headgroup. This corresponds to TSTP molecules interacting with the SDS

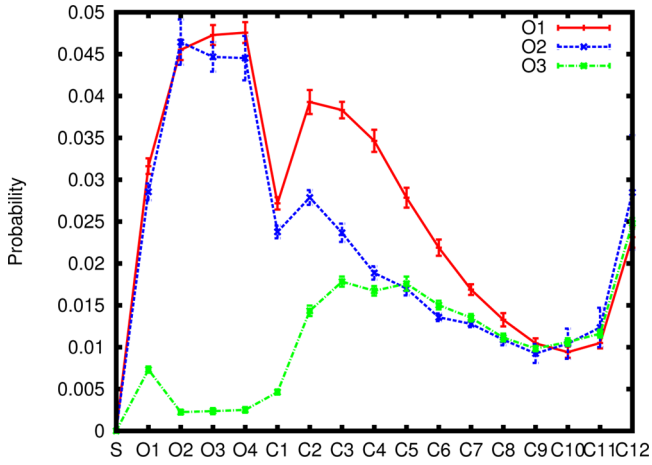

Figure 3. Probability distributions of the closest SDS heavy atoms to each oxygen atom on a TSTP molecule, which has adsorbed to the micelle's surface.

hydrocarbon tails which are situated within the interfacial region of the micelle (as is shown in Figure 2b) and do not represent TSTP molecules penetrating into the micelle core.

In order to characterize the interfacial interactions between the various molecular constituents of our micellar systems and the aqueous environments, we have calculated several different radial distribution functions, $g(r)$. Using the nearest neighbor distances, taken to be the distance corresponding to the first minimum in the $g(r)$ curve, we can also determine the average number of hydration water molecules around a given atom in a molecule by averaging the number of water molecules that are within the nearest neighbor distance from the $g(r)$, taking precautions not to double count any water molecules around the polar atoms in the SDS and/or TSTP molecules.

We identified the three oxygen atoms as the most prominent interaction sites in the TSTP molecule due to their increased polarity, and thus hydrogen bonding capabilities, compared to the nonpolar carbon rings. For this reason, we used the oxygen atoms in TSTP to probe interfacial properties of the drug. Radial distribution functions $[g(r)]$ between the oxygen atoms in the TSTP molecules and oxygen atoms in water molecules (OW) have been calculated and are presented in the Supporting Information. The O1-OW and O2-OW $g(r)$ curves show large sharp peaks between 2 and 3 Å, indicating that water molecules are hydrogen bonding to these oxygen atoms on the TSTP molecules; however, O3 has a small peak at a much larger distance (∼4.5 Å) that is probably due to the water molecules hydrogen-bonded to the O2 atom on the TSTP molecules. This is not surprising when one considers the position of O3 in the TSTP, it is less exposed than O1 and O2, and it has one more covalent bond, as shown in Figure 1b.

The number of hydrating water molecules around the O1, O2, and O3 atoms in the TSTP molecules were found to be 2.4 ± 1.1, 1.6 ± 0.8, and 2.2 ± 2.4, respectively. From these values alone, one might naively think that O3 is more hydrated than O2, which is counterintuitive. However, this is rationalized when we consider that the nearest neighbor distance of O3 is 2 Å larger than that of O2, and thus a larger volume is measured resulting in a misleadingly large hydration number. To put this into perspective, the number of hydration water molecules per unit volume (in Å^3) for O2 and O3 are 1×10^{-2} and 6×10^{-3}, respectively. Histograms of the number of hydration water molecules around the oxygen atoms in the TSTP molecule are

dx.doi.org/10.1021/jp508488c | J. Phys. Chem. B 2014, 118, 13192−13201

displayed in Figure 4 and show that the second most probable water hydration number for O3 is zero, further illustrating it is limited hydrogen-bonding capabilities.

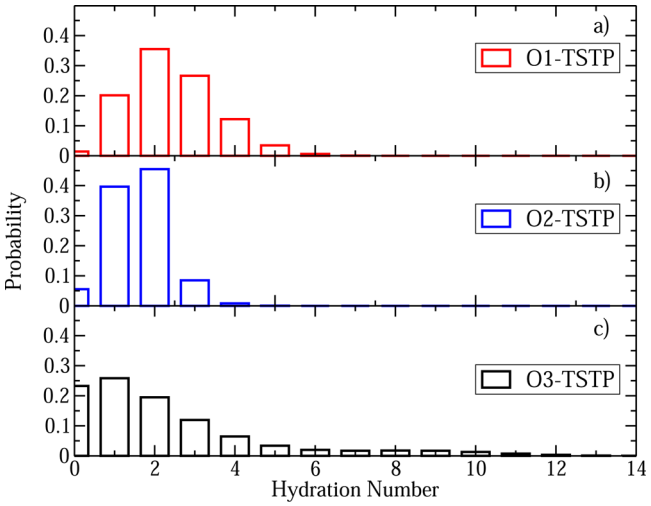

Figure 4. Histograms showing the fraction of (a) O1, (b) O2, and (c) O3 atoms in the adsorbed TSTP molecules that have a given hydration number.

To determine whether the TSTP molecules have a preferential orientation with respect to each other, we defined various segments of the TSTP molecule, which are shown in Figure 5a, and calculated the shortest displacements between these segments on nearest neighbor TSTP molecules. Then we determined the probability of each combination of segments being the closest.

Figure 5b reveals that the most probable segment pairing is 1 and 7, indicated by the red squares in opposite corners of the plot. This suggests that the TSTP molecules prefer to be

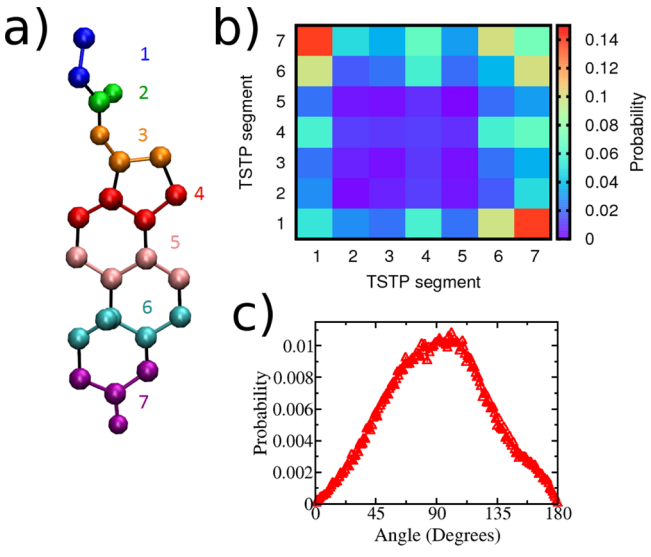

Figure 5. (a) Color-coded picture of the segments of the TSTP molecules that we have used to describe the association of TSTP molecules. (b) Histogram showing the probability that two neighboring TSTP molecules associate via a pair of segments as defined in (a). (c) Probability distribution of the angle formed by the vectors between O1 and O2 atoms in nearest neighbor TSTP molecules.

aligned in a head-to-tail fashion. In order to further understand the orientation of TSTP molecules with one another, we also calculated the angle formed by the vectors between O1 and O2 atoms in nearest neighbor TSTP molecules. Figure 5c shows a histogram of the angles found between nearest neighbor TSTP molecules and exhibits a broad curve centered at ~91°. Therefore, the preferred orientation of two TSTP molecules are such that they are aligned with the head of one molecule (segment 1) nearest to the tail (segment 7) of another molecule, and they are oriented such that there major axes are perpendicular to one another.

We observe from visual inspection that the TSTP molecules initially adsorb to the surface of the SDS micelle in a dense cluster, but as time evolves, they gradually start to migrate around the micelle until they are approximately evenly distributed around the shell. This is quantified by the plots in Figure 6, which show the TSTP center of mass location,

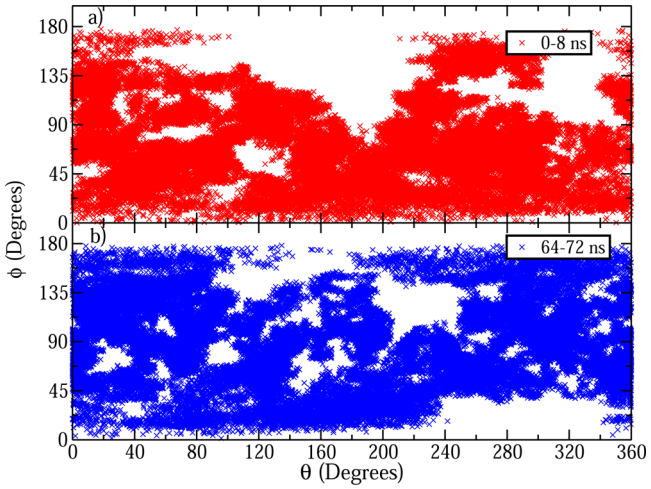

Figure 6. Plot of the location of the center of mass of the TSTP molecules as a function of the azimuthal θ and zenith ϕ angles around the surface of the micelle at (a) an initial part of the simulation (0–8 ns) and (b) toward the end of our simulation (64–72 ns).

described by (θ, ϕ), where θ and ϕ denote the azimuthal and zenith angles, respectively. θ is the projection onto the x–y plane of the vector from the origin to the center of mass of a TSTP molecule, this angle goes clockwise around the x–y plane from 0 to 360 deg. ϕ is the angle between the z axis and the vector to the center of mass of a TSTP molecule; this angle ranges from 0 to 180 deg, which corresponds to vectors pointing in the positive and negative z directions, respectively. Both θ and ϕ are measured relative to the micelle center of mass coordinate frame.

Figure 6a shows that initially the TSTP molecules are clustered in dense groups leaving large regions of the micelle's surface unpopulated. In particular, there is a large void at the top of the plot in the center, which corresponds to a large proportion of the bottom hemisphere of the micelle as pictured. Figure 6b reveals that in a later stage of the simulation, the blank regions of sampling are more disperse and the data points are more equally distributed over the zenith angles.

Effect of TSTP on SDS Micelle Shape and Structure. A variety of different physical quantities and distributions have been used to describe the structure of the micelles that we observe in our simulations. These various measures and their

dx.doi.org/10.1021/jp508488c | J. Phys. Chem. B 2014, 118, 13192–13201

results are described in this section, and Table 1 contains a summary of the results.

Table 1. Average Values of Various Structural Properties of the SDS and the SDS+TSTP Micelles Calculated from the Production Simulation Periods[a]

	SDS micelle	SDS + TSTP micelle
eccentricity	0.11 ± 0.07	0.16 ± 0.08
I_x/I_y	1.01 ± 0.17	1.03 ± 0.18
I_x/I_z	1.04 ± 0.20	1.18 ± 0.29
I_y/I_z	1.04 ± 0.18	1.15 ± 0.28
max l_x (Å)	48.06 ± 4.98	48.22 ± 5.81
max l_y (Å)	48.21 ± 4.37	49.75 ± 5.67
max l_z (Å)	49.18 ± 5.01	53.15 ± 6.06
SASA/molecule (Å^2)	169.9 ± 4.5	156.1 ± 4.2
total SASA (Å^2)	13592.8 ± 358.2	13734.9 ± 371.6
Voronoi surface area/molecule (Å^2)	149.7 ± 2.6	136.9 ± 2.2
total Voronoi surface area (Å^2)	11972.1 ± 206.6	12181.2 ± 193.5

[a]The quoted errors are one standard deviation of the data distributions.

The solvent accessible surface area (SASA) is a common method employed to calculate the surface area of complex molecular geometries. This is calculated by rolling a spherical probe, which is given a radius 1.4 Å to approximate a water molecule, over the van der Waals surface of the micelle and estimating the surface area. Plots of the SASA values for the SDS and SDS+TSTP micelle systems are shown in the Supporting Information. The SASA values remain stable during the simulations, indicating that the systems are in equilibrium throughout the majority of the production period. The average SASA per molecule for the SDS and the SDS+TSTP micelle systems is 169.91 Å^2/molecule and 156.08 Å^2/molecule, respectively. Note that the value for SASA/molecule calculated from the SDS+TSTP micelle includes contributions from the drug molecules, which are bound to the micelle surface. This was done in order not to report a value that could be misleading; if it were calculated merely from the SDS molecules it would include artificial voids from where the TSTP was located and therefore overestimate the SASA.

The SASA measurements are very sensitive to the size of the probe used, so in order to remove this dependence we have also calculated the surface area of the micelle systems using the Voronoi tesselation method implemented in the Voro++ software library that is integrated into LAMMPS.[42] This method constructs cells around the atoms where the segments of the Voronoi cell are all the points in the plane that are equidistant to the two nearest sites. The Voronoi vertices are the points equidistant to three (or more) sites. The surface areas determined from the Voronoi tesselation yielded smaller surface area values than those calculated with SASA as expected since the Voronoi surface areas will not be as sensitive to the roughness of the interface (see Table 1). Also, the Voronoi and SASA surface areas show that the surface area per molecule decreases with the inclusion of TSTP in the micelle. The Voronoi surface area was separated into contributions from head, tail, and TSTP regions of the micelle systems. From these measurements, we have determined that 42% of the surface area of the SDS micelle is due to headgroup atoms, while 58% of the surface area is due to the hydrocarbon tails. Whereas, in the SDS+TSTP micelle, 39%, 45%, and 16% of the surface area is due to the SDS head groups, SDS hydrocarbon chains, and TSTP molecules, respectively. The ratios of Voronoi surface area contributions of head-to-tail are 0.72 and 0.87 for the SDS and SDS+TSTP micelles, respectively. This suggests that the presence of TSTP, which sits in the same general position as the SDS headgroup, reduces the amount of the SDS hydrocarbon tail that is exposed to the aqueous environment.

In addition to studying the surface area of the micelles, we also studied the shape of the micelles. The micelle eccentricity provides a description of micelle shape and is defined as

$$\eta = 1 - \frac{I_{\text{min}}}{I_{\text{avg}}} \tag{1}$$

where I_{min} and I_{avg} denote the minimum and average moments of inertia of the micelle, respectively. When $\eta = 0$, the micelle is perfectly spherical, and as $\eta \rightarrow 1$ the micelle tends toward being infinitely oblong in shape. The eccentricity can also be used as a metric for micelle equilibration, when the micelle shape stabilizes the eccentricity will converge and exhibit small fluctuations around some value.

The eccentricity of the micelle was calculated for both simulations and output in 200 ps intervals. Plots of the eccentricity of the micelles in both of our simulations are presented in the Supporting Information. The micelle shape remains dynamic throughout the production periods in both simulations, which is suggested by the eccentricity values typically fluctuating between 0.01 and 0.3. The average eccentricity values indicate that while the SDS and SDS +TSTP micelles have the same general shape, the SDS+TSTP micelle is slightly less spherical in shape than the SDS micelle. This is also supported by the average values for the ratios of the moments of inertia of the micelles, which are slightly larger for the SDS+TSTP micelle in accordance to the larger average eccentricity. The average values for the maximum micelle dimensions in the x and y directions are very similar for both micelle systems; however, the maximum dimension in the z direction is 4 Å larger for the SDS+TSTP micelle.

A more detailed description of the internal micelle structure is obtained by measuring the density of various atomic species at a given displacement from the micelle center of mass. These distributions characterize the extent to which the density of atomic species fluctuates along the micelle radial axis, and they also provide some insight into the penetration depth of water, counterions, and drugs into the micelle core.

The density plots were determined by calculating the distance of selected atoms from the micelle center of mass in every snapshot and counting the number of atoms in 1 Å thick shells around the micelle center of mass. Figure 7 (panels a and b) shows the average density of the different chemical species that are found in SDS, water, and TSTP molecules. The plots reveal that the average micelle radius is approximately the same for both simulations, ∼2 nm which is consistent with a study conducted by Bruce et al.[11] on an SDS micelle with an aggregation number of 60. The average micelle radius is also consistent with the estimate provided by taking the average of the mean values for the maximum dimensions of the micelle in the x, y, and z directions which would give the diameter, and then dividing by two to get the radius.

The radial density plots generally show that the monomers are arranged such that the headgroups are in contact with the water, whereas the tails are contained in the micellar core

dx.doi.org/10.1021/jp508488c | J. Phys. Chem. B 2014, 118, 13192−13201

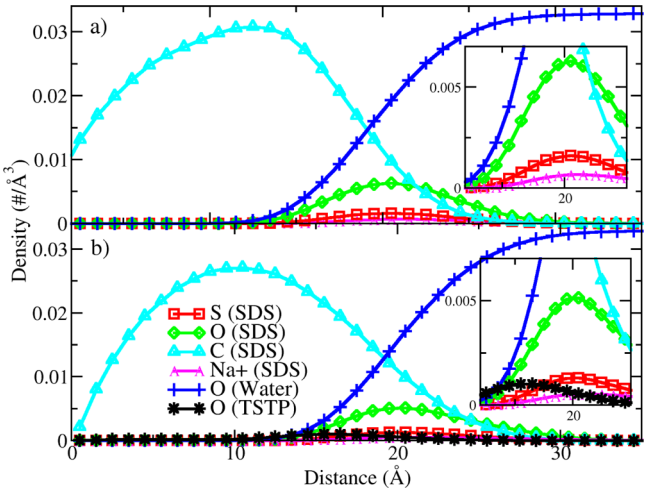

Figure 7. Radial density plots of the different chemical elements within the SDS, TSTP, and water molecules with respect to the center of mass of the (a) SDS and (b) SDS+TSTP micelles. The inset plots magnify the interfacial region of the plots for clarity. Note that the data labeled O(SDS) and O(TSTP) represent all oxygens in the SDS and TSTP molecules, respectively.

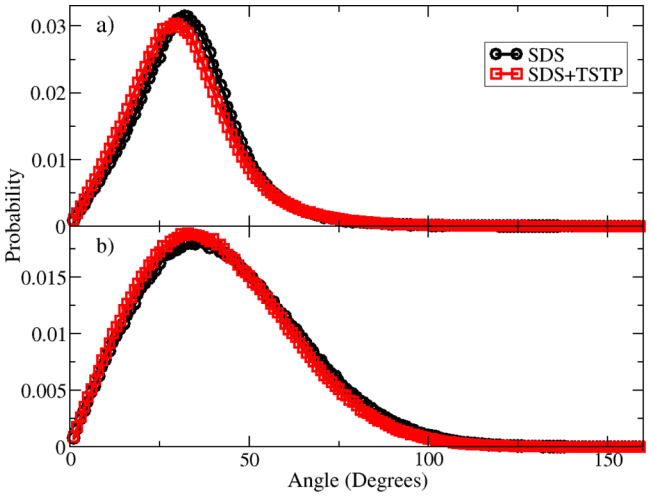

Figure 8. (a) Probability distributions of the angle formed between atoms C12 and C1 of the SDS molecule (as shown in Figure 1a) and the micelle center of mass for the SDS and SDS+TSTP micelle systems. (b) Probability distributions of the headgroup tilt angle formed between atoms S, O, and C12 in the SDS molecule (as shown in Figure 1a) for the SDS and SDS+TSTP micelle systems.

forming a hydrophobic environment. To quantify water penetration into the micelle core, we take the point at which the water density decays to 10% of that in the bulk, as was used by Bruce et al.[12] This method reveals water penetration of 14.5 and 15.5 Å away from the micelle center of mass for the SDS and SDS+TSTP micelles, respectively. In order to establish how much contact there is between the hydrocarbon tails and water in the micelles, we define a shell region: the distance between the point where water reaches 10% of its bulk density and the point where carbon decays to 10% of its peak density, which was also used by Bruce et al.[12] The size of these regions are 9 and 10 Å for the SDS micelle and the SDS+TSTP micelle, respectively. The oxygen atoms in TSTP have a very broad density distribution, the peak of which is visible in the inset plot in Figure 7b and is situated at 16.5 Å from the micelle center of mass.

Torsional effects arising from thermal fluctuations in the solvent can influence micellar structure by causing the surfactant tails to bend relative to some average position with respect to the micelle radial axis. The SDS chain angle distribution is a relatively simple method of determining how significant this torsional motion is to the micelle structure. We define the SDS chain angle as the angle between the vectors formed between C1 (the headgroup carbon) and the micelle center of mass (COM), and the vector connecting C12 (the carbon of the terminal methyl group) and the micelle COM. When this angle is zero, the chain is aligned perfectly along the micelle radial axis and when this angle is 90°, the SDS molecule has been dislodged from the micelle structure and the chain is at a tangent to the micellar surface. The chain angle distributions were produced by calculating the angle between the vectors defined above for every SDS molecule in every snapshot of the trajectory and binning the observed angles to produce histograms. The SDS chain angle distributions for both simulations are shown in Figure 8a and reveal that the mean chain angles for the SDS and SDS+TSTP micelles are 33.1° and 31.8°, respectively. Therefore, the presence of TSTP causes no statistical difference between the mean chain angle distributions calculated for the micelles.

We also calculated the angle distribution for the SDS headgroup tilt, which is defined as the angle between the vector formed between S (the sulfur atom in the SDS headgroup) and C1 atoms and the vector formed between C1 and C12 atoms. When this angle is zero, the entire molecule is aligned linearly and when this angle is 90° the headgroup is oriented such that it is perpendicular to the SDS hydrocarbon chain. Figure 8b shows that the presence of TSTP has almost no effect on the distribution of the headgroup tilt angle either. The mean headgroup tilt angles are almost equal at 42.9° and 41.1° for the SDS and the SDS+TSTP micelles, respectively.

Effect of TSTP on SDS Micelle Interfacial Properties. In this section, we present how the presence of TSTP affects the interfacial properties of the micelles. In order to do so, we have calculated a variety of $g(r)$'s to describe the interactions between the SDS molecules and their aqueous environments, and these are shown in the Supporting Information. From these $g(r)$'s we are able to determine the nearest neighbor distance from the location of the first minimum in the $g(r)$ curve.

The nearest neighbor distance for the oxygen and hydrogen atoms of the water molecules around the sulfur atoms in the SDS headgroup remains unchanged in the presence of TSTP. The calculated nearest neighbor distances for S-OW and S-HW are 4.8 and 3.5 Å, respectively, which are consistent with other values calculated from similar studies of SDS micelles.[20] This also shows that the interfacial water molecules orient themselves such that the hydrogen atoms are closer to the surfactant head groups than oxygen.

Figure 9 shows histograms of the number of hydration water molecules for the two micelle systems. The distributions are almost identical, suggesting that the presence of TSTP does not affect the hydrogen bonding network around the interfacial region, and this is confirmed by the mean number of hydration water molecules around S which are 9.1 ± 2.3 and 9.2 ± 2.3 for the SDS and the SDS+TSTP micelle systems, respectively. Both histograms exhibit broad distributions ranging from 2 to 15 water molecules per sulfur atom. We further investigated the interfacial hydration properties by calculating the hydration number distributions for O4 in SDS (the oxygen atom bound

dx.doi.org/10.1021/jp508488c | J. Phys. Chem. B 2014, 118, 13192−13201

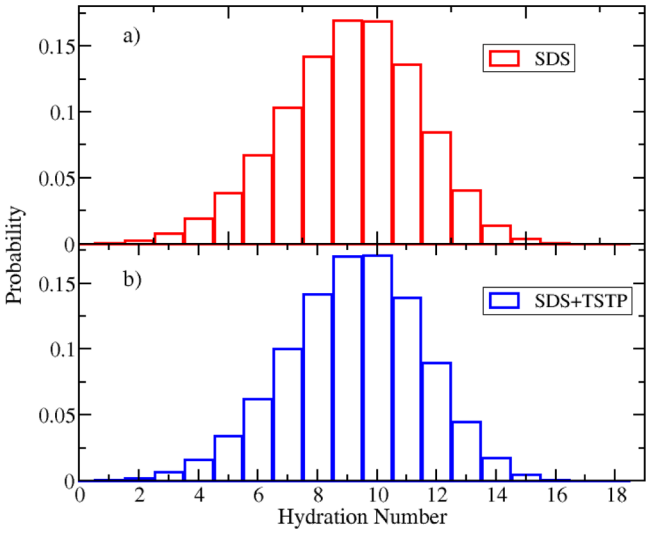

Figure 9. Histograms showing the probability that a sulfur atom in the SDS headgroup has a given hydration number for (a) the SDS and (b) SDS+TSTP micelle.

to sulfur and C1) and comparing them for both simulations. There is no significant difference between the distributions with and without TSTP, so that means that the hydration of the entire headgroup is unaffected by the presence of TSTP.

To study the interfacial behavior of the counterions, we calculated the $g(r)$'s between the sulfur atoms in the SDS headgroup and the sodium counterions of SDS for both simulations; the resulting plots are shown in the Supporting Information. We define ion shells to exist around the sulfur atoms at the distances at which the minimums in the $g(r)$ curves occur. The first and second shells of sodium ions are located at 4.2 and 6.8 Å, respectively, and these values are in exact agreement with the study conducted by Bruce et al.[11]

Comparing the abundance of sodium ions in the first and second ion shells in both simulations revealed that the occupation of ions was similar for both systems but slightly less for the SDS+TSTP micelle. For the SDS micelle, we found that 21% of the sodium ions occupy the first shell, while 48% were contained within the first two shells. For the SDS+TSTP micelle, 17% were situated in the first shell while 43% were found in the first two shells. To establish how the TSTP affects the local concentration of ions, we compared the distribution of sodium ions within the nearest neighbor distance of the sulfur atoms that were closest and furthest away from any TSTP molecule for every simulation snapshot. We found a higher probability (0.31) that one of the sulfur atoms closest to the TSTP molecules have 1 or 2 sodium counterions bound to them is significantly larger than for the sulfur atoms which were furthest away (0.14). For comparison, we found that the probability of a sulfur atom being bound to 1 or 2 Na^+ counterions is 0.19 in the SDS micelle. Therefore, it appears that TSTP molecules attract the Na^+ counterions. Consulting the $g(r)$ curves between Na^+ and the oxygen atoms in the TSTP molecules, there are very prominent first neighbor peaks for the O1−Na^+ and O2−Na^+ interactions at a distance of ∼3.0 Å.

CONCLUSIONS

Atomistic molecular dynamics simulations were used to investigate the structural and interfacial properties of SDS micelles with and without the presence of TSTP. These micelles were created using the aggregation numbers found from our recent neutron scattering data, which is different from the aggregation number of 60 that has been previously used in most simulation studies of SDS micelles in aqueous environments, which is summarized in the Supporting Information. Also, we have taken care to carry out our simulations at the same concentration of the SDS as was used experimentally, therefore, reproducing the experimental system as accurately as possible.

The structural properties of the SDS micelle that we calculated for our system are consistent with those that have been published previously for micelles consisting of different numbers of SDS molecules. We observed that our micelle was slightly nonspherical with an average eccentricity of 0.11, which is nearly identical to the values reported for micelles consisting of 60 SDS molecules[11,13,19,22] and is a bit smaller but within error of the value reported by Palazzesi et al.[14] The earlier simulations that showed more spherical micelles were very short simulations and so the shape of the micelle most likely had not equilibrated.[9,10]

The surface area of the SDS micelle that we simulated (SASA: ∼170 Å^2/molecule, Voronoi: ∼150 Å^2/molecule) is comparable to the values obtained from other recent simulation studies of SDS micelles containing 60 molecules in an aqueous environment, including 176 Å^2/molecule[11] and 147 Å^2/molecule.[14] However, in our systems which have a larger aggregation number than the micelle studied by Bruce et al., we found a larger amount of the surface area consists of hydrocarbon atoms at the interface (58%) than was found by Bruce et al. (∼30%).[12]

The interfacial properties of the SDS properties reported in this manuscript are consistent with those found in other MD simulation studies of similar systems. The hydration numbers that we found for the sulfur atom in the headgroup of the SDS molecules (∼9.1) is nearly identical to that found by Rakitin and Pack (∼9.4)[13] and is only slightly larger than that found by Sammalkorpi et al. (∼8.0) who studied the self-assembly of micelles and therefore had a distribution of micelle sizes within their system.[20]

Additionally, the amount of Na^+ counterions found in the first neighbor shell and second neighbor shell around the sulfur atom in the SDS headgroup is consistent with the majority of other simulation studies.

Additionally, the number of Na^+ counterions found within the distances corresponding to the first and second minima in the $g(r)$ curves between Na^+ counterions and the sulfur atoms in the SDS headgroup is consistent with the majority of other simulation studies.[11,13,16] Meanwhile, Sammalkorpi et al. found a significantly smaller proportion of Na^+ counterions bound to the sulfur atoms of the headgroup,[20] but Palazzesi et al. found a significantly larger proportion of bound Na^+ ions.[14] This is not too surprising as this seems to be the most variable interaction observed when using different force fields for the simulation.[21]

We observe only slight changes to the structural and interfacial properties of a SDS micelle in the presence of TSTP as compared to the same properties of a SDS micelle on its own. The SDS+TSTP micelle is slightly less spherical and also increases in size as compared to that with only SDS. However, the surface area per molecule decreases by ∼9%. There is no significant change observed in the orientation of the chains within the micelle as a result of this increase in size.

dx.doi.org/10.1021/jp508488c | J. Phys. Chem. B 2014, 118, 13192−13201

We observe that the TSTP molecules preferentially sit on the micelle surface and interact with the polar SDS head groups. In some instances they seem to interact with carbons on the hydrocarbon chain of SDS that are at the surface of the micelle. Even though the TSTP is found at the interface, it has no observable effect on the hydration of the headgroup of the SDS molecules in the micelle. However, there seems to be a correlation between the distribution of the Na^+ counterions at the micelle's surface and the location of the TSTP on the surface.

We have observed that a SDS headgroup which is closest to a TSTP molecule is twice as likely to be bound to less than 2 Na^+ counterions than a SDS headgroup which is furthest away from the TSTP molecules.

Additionally, we observe that after the TSTP adsorb onto the surface of the micelle, they are able to diffuse along the surface of the micelle in order to find preferential locations with relation to one another on the micelle's surface. In doing so, the TSTP appear to prefer to be more or less equally spaced on the micelle's surface.

In this paper, we have developed a detailed description of the solubilization of TSTP by a SDS micelle, and in doing so, we have characterized the interfacial properties of the SDS micelle and how it changes with TSTP present. We have determined that the TSTP is found in the headgroup region of the SDS molecules at the interface between the micelle and the aqueous environment. We believe that this is due to the competition between the polar oxygen groups on the TSTP molecule interacting with the aqueous environment and the hydrophobic parts of the TSTP molecule interacting favorably with the hydrocarbon chains of the SDS molecules. The initial findings of our simulations of TSTP interacting with SDS monolayers seem to provide further evidence for this competition of interactions.

In the future, we plan to gain an understanding of how the chemical nature of the drug and surfactant molecule effect the solubilization process. In this system, it seems that the Na^+ counterion which localize around the TSTP molecules found at the micelle's surface are playing a role in the stabilization of the TSTP molecules interacting with the SDS molecules. We will further test this hypothesis by studying micelles made up of different surfactant molecules, as well as changing the chemical composition of the drug molecule and the concentration of ions in the aqueous environment.

Additionally, we plan to study the dynamics of the self-assembly and encapsulation processes. For this later work, due to the challenges posed by studying these systems with atomistic simulations,[43] we plan to develop a coarse-grain model for the surfactants and drug molecules.

■ ASSOCIATED CONTENT

Supporting Information

(i) A brief description of the neutron experiments and the data obtained from them which is used to provide a starting state for the simulations presented in this manuscript; (ii) plots of structural measures of the surface area and shape of the SDS and SDS+TSTP micelles; (iii) radial distribution functions of the interactions between the sulfur atoms in the SDS headgroup and the water and counterions in solution; and (iv) the movement of the TSTP along the surface of the SDS micelle. This material is available free of charge via the Internet at http://pubs.acs.org.

■ AUTHOR INFORMATION

Corresponding Author

*E-mail: chris.lorenz@kcl.ac.uk.

Notes

The authors declare no competing financial interest.

■ ACKNOWLEDGMENTS

D.T.A. and C.D.L. thank the EPSRC for the GTA studentship which funds DTA's research. Y.S. and M.J.L. thank the GETFund (Ghana Education Trust Fund) for funding the Ph.D. studentship of Y.S.

■ REFERENCES

(1) Lawrence, M. J.; Rees, G. D. Microemulsion-Based Media as Novel Drug Delivery Systems. *Adv. Drug Delivery Rev.* **2000**, *45*, 89−121.

(2) Rabinow, B. E. Nanosuspensions in Drug Delivery. *Nat. Rev. Drug Discovery* **2004**, *3*, 785−796.

(3) Mishra, B.; Patel, B. B.; Tiwari, S. Colloidal Nanocarriers: A Review on Formulation Technoloy, Types and Applications Toward Targeted Delivery. *Nanomed. Nanotechnol. Bio. Med.* **2010**, *6*, 9−24.

(4) Krishna, A. K.; Flanagan, D. R. Micellar Solubilization of a New Antimalarial Drug *β*-arteether. *J. Pharm. Sci.* **1989**, *78*, 574−576.

(5) Rangel-Yagui, C. O.; Hsu, H. W. L.; Pessua, A. J.; Costa Tavares, L. Micellar Solubilization of Ibuprofen: Influence of Surfactant Head Groups on the Extent of Solubilization. *Braz. J. Pharm. Sci.* **2005**, *41*, 237−246.

(6) Mall, S.; Buckton, G.; Rawkins, D. A. Dissolution Behaviour of Sulphonamides into Sodium Dodecyl Sulfate Micelles: A Thermodynamic Approach. *J. Pharm. Sci.* **1996**, *85*, 75−78.

(7) Göktürk, S.; Aslan, S. Study on Binding Properties of Poorly Soluble Drug Trimethoprim in Anionic Micellar Solutions. *J. Dispersion Sci. Technol.* **2014**, *35*, 84−92.

(8) Enache, M.; Anghelache, I.; Volanschi, E. Coupled Spectral and Electrochemical Evaluation of the Anticancer Drug Mitoxantrone-Sodium Dodecyl Sulfate Interaction. *Int. J. Pharm.* **2010**, *390*, 100−106.

(9) Shelley, J.; Watanabe, K.; Klein, M. L. Simulation of a Sodium Dodecylsulfate Micelle in Aqueous Solution. *Int. J. Quantum Chem.* **1990**, *17*, 103−117.

(10) MacKerell, A. D. J. Molecular Dynamics Simulation Analysis of a Sodium Dodecyl Sulfate Micelle in Aqueous Solution: Decreased Fluidity of the Micelle Hydrocarbon Interior. *J. Phys. Chem.* **1995**, *99*, 1846−1855.

(11) Bruce, C. D.; Berkowitz, M. L.; Perera, L.; Forbes, M. D. E. Molecular Dynamics Simulation of Sodium Dodecyl Sulfate Micelle in Water: Micellar Structural Characteristics and Couterion Distribution. *J. Phys. Chem. B* **2002**, *106*, 3788−3793.

(12) Bruce, C. D.; Senepati, S.; Berkowitz, M. L.; Perera, L.; Forbes, M. D. E. Molecular Dynamics Simulation of Sodium Dodecyl Sulfate Micelle in Water: Micellar Structural Characteristics and Couterion Distribution. *J. Phys. Chem. B* **2002**, *106*, 10902−10907.

(13) Rakitin, A. R.; Pack, G. R. Molecular Dynamics Simulations of Ionic Interactions with Dodecyl Sulfate Micelles. *J. Phys. Chem. B* **2004**, *108*, 2712−2716.

(14) Palazzesi, F.; Calvaresi, M.; Zerbetto, F. A Molecular Dynamics Investigation of Structure and Dynamics of SDS and SDBS Micelles. *Soft Matter* **2011**, *7*, 9148−9156.

(15) Gao, J.; Ge, W.; Hu, G.; Li, J. From Homogeneous Dispersion to Micelles: A Molecule Dynamics Simulation on the Compromise of the Hydrophilic and Hydrophobic Effects of Sodium Dodecyl Sulfate in Aqueous Solutions. *Langmuir* **2005**, *21*, 5223−5229.

(16) Yoshii, N.; Okazaki, S. A Molecular Dynamics Study of Surface Structure of Spherical SDS Micelles. *Chem. Phys. Lett.* **2006**, *426*, 66−70.

(17) Jalili, S.; Akhavan, M. A Coarse-Grained Molecular Dynamics Simulation of a Sodium Dodecyl Sulfate Micelle in Aqueous Solution. *Colloids Surf., A* **2009**, *352*, 99−102.
(18) Sammalkorpi, M.; Karttunen, M.; Haataja, M. Ionic Surfactant Aggregates in Salene Solutions: Sodium Dodecyl Sulfate in the Presence of Excess Sodium Chloride (NaCl) or Calcium Chloride ($CaCl_2$). *J. Phys. Chem. B* **2009**, *113*, 5863−5870.
(19) Yoshii, N.; Okazaki, S. A Molecular Dynamics Study of Structural Stability of Spherical SDS Micelle as a Function of its Size. *Chem. Phys. Lett.* **2006**, *426*, 58−61.
(20) Sammalkorpi, M.; Karttunen, M.; Haataja, M. Structural Properties of Ionic Detergent Aggregates: A Large-Scale Molecular Dynamics Study of Sodium Dodecyl Sulfate. *J. Phys. Chem. B* **2007**, *111*, 11722−11733.
(21) Tang, X.; Koenig, P. H.; Larson, R. G. Molecular Dynamics Simulations of Sodium Dodecyl Sulfate Micelles in Water: The Effect of the Forcefield. *J. Phys. Chem. B* **2014**, *118*, 3864−4880.
(22) Yan, H.; Cui, D.; Bu-Liu, C.; Yuan, S.-L. Molecular Dynamics Simulations of Pyrene Solubilized in a Sodium Dodecyl Sulfate Micelle. *Langmuir* **2011**, *28*, 4931−4938.
(23) Schwarze, M.; Volovych, I.; Wille, S.; Mokrushina, L.; Arlt, W.; Schomcäcker, R. Partition Coefficients of Itaconates in Aqueous Micellar Solutions: Measurements and Predictions with COSMO-RS. *Ind. Eng. Chem. Res.* **2012**, *51*, 1846−1852.
(24) Storm, S.; Jakobtorweihen, S.; Smirnova, I.; Panagiotopoulos, A. Z. Molecular Dynamics Simulation of SDS and CTAB Micellization and Prediction of Partition Equilibria with COSMOmic. *Langmuir* **2013**, *29*, 11582−11592.
(25) Martinez, L.; Andrade, R.; Birgin, E. G.; Martinez, J. M. Packmol: A Package for Building Initial Configurations for Molecular Dynamics Simulations. *J. Comput. Chem.* **2009**, *30*, 2157−2164.
(26) Lorenz, C. D.; Hsieh, C.-M.; Dreiss, C. A.; Lawrence, M. J. Molecular Dynamics Simulations of the Interfacial and Structural Properties of Dimethyldodecylamine-*N*-oxide Micelles. *Langmuir* **2011**, *27*, 546−553.
(27) Plimpton, S. Fast Parallel Algorithms for Short-Range Molecular Dynamics. *J. Comput. Phys.* **1995**, *117*, 1−19.
(28) Vanommeslaeghe, K.; Hatcher, E.; Acharya, C.; Kundu, S.; Zhong, S.; Shim, J.; Darian, E.; Guvench, O.; Lopes, P.; Vorobyov, I.; Makerell, A. D. J. CHARMM General Force Field (CGenFF): A Force Field for Drug-like Molecules Compatible with the CHARMM All-Atom Additive Biological Force Fields. *J. Comput. Chem.* **2010**, *31*, 671−690.
(29) Yu, W.; Vanommeslaeghe, K.; MacKerell, A. D. J. Extension of the CHARMM General Force Field to Sulgonyl-Containing Compounds and its Utility to Biomolecular Simulations. *J. Comput. Chem.* **2012**, *33*, 2451−2468.
(30) Klauda, J. B.; Venable, R. M.; Freites, J. A.; O' Connor, J. W.; Tobias, D. J.; Mondragon-Ramirez, C.; Vorobyov, I.; MacKerell, A. D. J.; Pastor, R. W. Update of the CHARMM All-Atom Additive Force Field for Lipids: Validation on Six Lipid Types. *J. Phys. Chem. B* **2010**, *114*, 7830−7843.
(31) Pastor, R. W.; MacKerell, A. D. J. Development of the CHARMM Force Fields for Lipids. *J. Phys. Chem. Lett.* **2011**, *2*, 1526−1532.
(32) Jorgensen, W. L.; Chandrasekhar, J.; Madura, J. D.; Impey, R. W.; Klein, M. L. Comparison of Simple Potential Functions for Simulating Liquid Water. *J. Chem. Phys.* **1983**, *79*, 926−935.
(33) Reiher, W. I. *Theoretical Studies of Hydrogen Bonding*. Ph.D. dissertation, Harvard University, 1985.
(34) Hockney, R. W.; Eastwood, J. W. Computer Simulation using Particles. *J. Chem. Phys.* **1983**, *79*, 926−935.
(35) Parrinello, M.; Rahamn, A. Polymorphic Transitions in Single Crystals: A New Molecular Dynamics Method. *J. Appl. Phys.* **1981**, *52*, 7182−7190.
(36) Martyna, G. J.; Tobias, D. J.; Klein, M. L. Constant Pressure Molecular Dynamics Algorithms. *J. Chem. Phys.* **1994**, *101*, 4177−4189.
(37) Shinoda, W.; Shiga, M.; Mikami, M. Rapid Estimation of Elastic Constants by Molecular Dynamics Simulation under Constant Stress. *Phys. Rev. B* **2004**, *69*, 134103.
(38) Tuckerman, M. E.; Alejandre, J.; López-Rendón, R.; Jochim, A. L.; Martyna, G. J. A Lioville-Operator Derived Measure-Preserving Integrator for Molecular Dynamics Simulations in Isothermal-Isobaric Ensemble. *J. Phys. A: Math. Gen.* **2006**, *39*, 5629−5651.
(39) Hoover, W. G. Canonical Dynamics: Equilibrium Phase-Space Distributions. *Phys. Rev. A* **1985**, *31*, 1695−1697.
(40) Hoover, W. G. Constant-Pressure Equations of Motion. *Phys. Rev. A* **1986**, *34*, 2499−1697.
(41) Ryckaert, J. P.; Ciccotti, G.; Berendsen, H. J. C. Numerical Integration of the Cartesion Equations of Motion of a System with Constraints: Molecular Dynamics of *n*-Alkanes. *J. Comput. Phys.* **1977**, *23*, 327−341.
(42) Rycroft, C. H. Voro++: A Three-Dimensional Voronoi Cell Library in C++. *Chaos* **2009**, *19*, 041111.
(43) Jusufi, A. Molecular Simulations of Self-Assembly Processes of Amphiphiles in Dilute Solutions: The Challenge for Quantitative Modelling. *Mol. Phys.* **2013**, *111*, 3182−3192.